Journal of Applied Electrochemistry **33**: 917–927, 2003.

Electrochemical oxidation of several chlorophenols on diamond electrodes Part I. Reaction mechanism☆

P. CAÑIZARES, J. GARCÍA-GÓMEZ, C. SÁEZ and M.A. RODRIGO*
Departamento de Ingeniería Química, Facultad de Ciencias Químicas, Universidad de Castilla La Mancha, Campus Universitario s/n., 13071 Ciudad Real, Spain
*(*author for correspondence, e-mail: Manuel.Rodrigo@uclm.es)*

Received 17 October 2002; accepted in revised form 20 March 2003

Key words: boron-doped diamond, chlorophenols, electrochemical oxidation, wastes

Abstract

The electrochemical oxidation of 4-chlorophenol, 2,4-dichlorophenol and 2,4,6-trichlorophenol aqueous wastes using boron-doped diamond electrodes was studied. This treatment led to complete mineralization of the wastes regardless of the operating conditions. A simple mechanistic model is consistent with the voltammetric and electrolysis results. According to this model, the electrochemical treatment of chlorophenol aqueous wastes involves the anodic and cathodic release of chlorine followed by the formation of non-chlorinated aromatic intermediates. Subsequent cleavage of the aromatic ring gives rise to non-chlorinated carboxylic acids. Chlorine atoms arising from the hydrodehalogenation of the chlorophenols are converted into more oxidized molecules at the anode. These molecules react with unsaturated C_4 carboxylic acid to finally yield trichloroacetic acid through a haloform reaction. The non-chlorinated organic acids are ultimately oxidized to carbon dioxide and the trichloroacetic acid into carbon dioxide and volatile organo-chlorinated molecules. Both direct and mediated electrochemical oxidation processes are involved in the electrochemical treatment of chlorophenols.

1. Introduction

Chlorinated phenols are present in wastewaters arising from a variety of industries. Most of these compounds are highly toxic and are suspected carcinogens, as well as having activity as environmental endocrine disrupters [1]. It has been reported [2] that the toxicity of chlorophenols increases with the number of chloro-substituents but is lowered by the presence of chloro-substituents in the *ortho*-position (Table 1). An increase in the number of chloro-substituents can also promote the accumulation of such chemical compounds in fish and other organisms [3], thus increasing their hazardous properties.

A number of studies have been carried out on the electrochemical oxidation of chlorophenol aqueous wastes using different kinds of anode [4–13]. In each case almost total mineralization of the organic compounds was achieved. This fact confirms electrochemical oxidation to be one of the most promising techniques for the treatment of wastewater containing small amounts of organo-chlorinated aromatic compounds.

Nevertheless, this technology is not currently applied commercially, mainly due to the high energy consumption associated with it. The high operating costs are due to the large number of electrons needed to completely oxidize organic matter to carbon dioxide. Partial oxidation of pollutants to obtain wastes that can be biologically treated (in a combined process) requires less energy, but it is important to consider that some intermediates may also be toxic and such materials must be completely removed [14].

In the search for less expensive applications it is important to have a good understanding of the process. Unfortunately, the mechanisms involved in the electrochemical oxidation of chlorophenols are complex and are not yet fully understood. The intermediates obtained in the electrochemical oxidation of these compounds depend on the particular chlorophenol oxidized, the anode material and the operating conditions. These intermediates are commonly quinones, carboxylic acids formed by oxidation and polymers formed by coupling of radicals generated during the process. Some intermediates are chlorinated whereas others are not, indicating the existence of mechanisms involving chlorine elimination. Normally the non-chlorinated intermediates are less toxic than the chlorinated ones (which can be even more toxic than the initial chlorophenol).

☆This paper was originally presented at the 6th European Symposium on Electrochemical Engineering, Düsseldorf, Germany, September 2002.

Table 1. Toxicity of phenol and several chlorophenols [1] based on 96 h LC_{50} values for fathead minnow (concentration units of the chemicals are mol dm^{-3})

Compound (CAS no.)	$-\log (LC_{50})$
Phenol (108-95-2)	3.50
o-chlorophenol (95-57-8)	4.00
p-chlorophenol (106-48-9)	4.46
2,4-dichlorophenol (120-83-2)	4.30
2,4,6-trichlorophenol (88-06-2)	4.64
2,3,4,6-tetrachlorophenol (58-90-2)	5.35
pentachlorophenol (87-86-5)	6.04

The work described here concerns a study of the electrochemical oxidation process for three chlorophenols (CP) on boron-doped diamond (BDD) electrodes: 4-chlorophenol (MCP), 2,4-dichlorophenol (DCP) and 2,4,6-trichlorophenol (TCP). The aim of the work was to elucidate mechanistic aspects of the oxidation process through a voltammetric and galvanostatic electrolysis study.

2. Experimental details

2.1. *Analytical procedures*

The carbon concentration was monitored using a Shimadzu TOC-5050 analyser. Carboxylic acids were monitored using a Supelcogel H column (mobile phase, 0.15% phosphoric acid solution; flowrate, 0.15 ml min^{-1}). The u.v. detector was set at 210 nm. Aromatics were monitored using a Nucleosil C_{18} column (mobile phase 40% water/60% acetonitrile; flowrate 0.50 ml min^{-1}). In this case the u.v. detector was set to 270 nm. Volatile chlorinated compounds were identified by gas chromatography and quantified by mass balance. Inorganic ions were measured by ion chromatography (column, Metrosep Anion Dual 2; mobile phase 1.3 mM Na_2CO_3 and 2.0 mM $NaHCO_3$; flowrate 0.80 ml min^{-1}).

2.2. *Electrochemical cell*

The oxidation of chlorophenols was carried out in a single-compartment electrochemical flow cell (Figure 1). Diamond-based materials were used as anodes and stainless steel (AISI 304) as the cathode. Both electrodes were circular (100 mm dia.) with a geometric area of 78 cm^2 each and an electrode gap of 9 mm. The electrolyte was stored in a glass tank (500 ml) and circulated through the electrolytic cell by means of a centrifugal pump. A heat exchanger was used to maintain the temperature at the desired set point. The experimental setup also contained a cyclone for gas deabsorption, and a gas absorber to collect the carbon dioxide and chlorine contained in the gases evolved from the reactor into sodium hydroxide.

2.3. *Diamond electrode preparation*

Boron-doped diamond films were synthesised by the hot filament chemical vapour deposition technique (HF CVD) on single-crystal p-type Si ⟨100⟩ wafers (0.1 Ω cm, Siltronix). The temperature range of the filament was 2440–2560 °C and that of the substrate was 830 °C. The reactive gas was methane in excess dihydrogen (1% CH_4 in H_2). The dopant gas was trimethylboron with a concentration of 3 mg dm^{-3}. The gas mixture was supplied to the reaction chamber at a flow rate of 5 dm^3 min^{-1}, giving a growth rate of 0.24 $\mu m\ h^{-1}$ for the diamond layer. The resulting diamond film thickness was about 1 μm. This HF

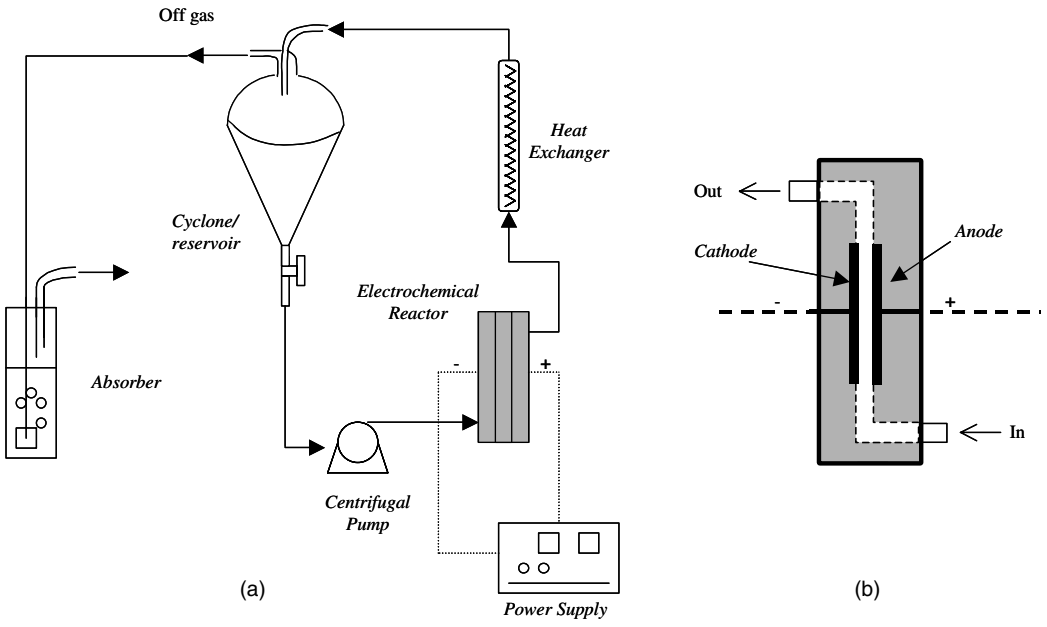

Fig. 1. Layout of the pilot plant. Detail of the electrochemical cell section.

CVD process produces columnar, random texture, polycrystalline films.

2.4. *Voltammetry experiments*

Electrochemical measurements were obtained using a conventional three-electrode cell in conjunction with a computer-controlled potentiostat/galvanostat (model PGP 201, Voltalab 21, Radiometer, Copenhagen). Diamond and stainless steel (AISI 304) were used as the working electrodes, $Hg/Hg_2Cl_2 \cdot KCl$ (sat) as a reference and stainless steel (AISI 304) as a counter electrode. Voltammetry experiments were performed in unstirred solutions. Anodes were anodically polarized prior to each experiment.

2.5. *Galvanostatic electrolysis*

Galvanostatic electrolyses were carried out to determine the main intermediates formed in the process. The average composition of the wastewater used in the experiments was 1.10 mmol dm^{-3} of the chlorophenol (MCP, DCP and TCP), 5000 mg Na_2SO_4 dm^{-3} and H_2SO_4 in suitable amounts to give a pH of 2 (or NaOH to reach a pH of 12). The pH was kept constant by the continuous introduction of sulfuric acid (or sodium hydroxide) to the electrolyte reservoir. In several experiments aimed at determining the influence of the initial organic matter concentration, the organic concentration was increased to 27.80 mmol dm^{-3} (except for TCP owing to its low solubility). The cell potential was constant during each electrolysis, indicating that appreciable deterioration of the electrode or passivation phenomena did not take place. The electrolyte flow rate through the cell was 1250 cm^3 min^{-1}.

3. Results and discussion

3.1. *Voltammetric study*

Linear sweep voltammograms with BDD electrodes of solutions containing 1.10 mM of MCP, DCP or TCP, and 5000 mg dm^{-3} of Na_2SO_4 at pH 2 (sulfuric acid) are shown in Figure 2. The curve obtained under the same experimental conditions but without CPs is also shown for the sake of comparison. The presence of CPs leads to the appearance of two anodic oxidation peaks in each case. The first peak (p1) is in the typical potential region for the oxidation of phenols (1.3–1.4 V vs SCE). The second peak (p2) is very close to the oxygen evolution region (2.2–2.4 V vs SCE) and is partially overlapped by this side reaction. Despite the appearance of this second peak potential, other differences could not be observed in the oxygen evolution region. The first peak decreased in size as the number of chloro-substituents in the CP molecule increased, while the second peak seemed to increase.

The effect of pH on the anodic oxidation processes of MCP is shown in Figure 3(a). A new anodic oxidation peak (p3) appears at alkaline pH (0.70 V vs SCE). Likewise, the oxygen evolution at alkaline pH shifted to the left and became slower. Reverse peaks were not observed, which indicates the occurrence of irreversible processes. The new anodic oxidation peak can also be observed in voltammograms for DCP and TCP (Figure 3(b)).

Cyclic voltammograms for MCP in acidic and alkaline media are shown in Figure 4. All the oxidation peaks decreased in size after the first scan, especially peaks p1 and p3, which almost disappeared completely. The influence of the scan rate on the electrochemical oxidation of MCP is represented in Figure 5. The three

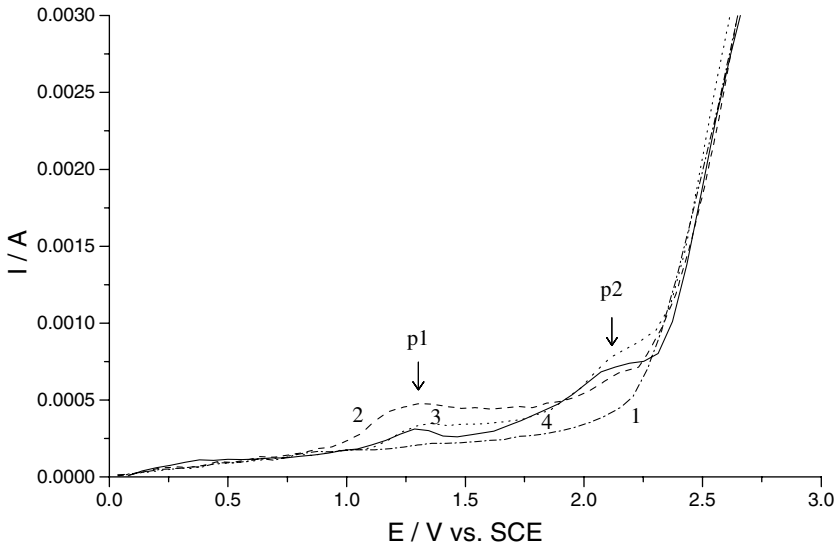

Fig. 2. Linear sweep voltammograms on BDD anodes of sulfuric acid/sodium sulfate solutions (5000 mg dm^{-3} Na_2SO_4; pH 2) containing: (1) no organic matter; (2) 1.10 mM of MCP; (3) 1.10 mM of DCP and (4) 1.10 mM of TCP. Scan rate 50 mV s^{-1}. Auxiliary electrode: Stainless steel AISI 304. Reference electrode: SCE.

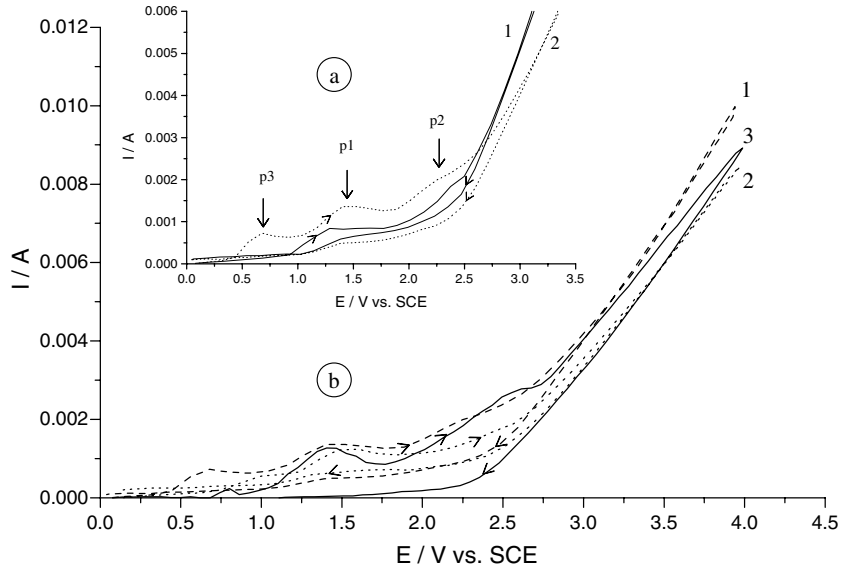

Fig. 3. Influence of pH on the anodic oxidation of CP. (a) Cyclic voltammograms (first cycle) on BDD anodes of MCP solutions (500 mg dm^{-3}) on sodium sulfate media at pH 2 (1) and pH 12 (2). Scan rate 100 mV s^{-1}. Auxiliary electrode: Stainless steel AISI 304. Reference electrode: SCE. (b) Cyclic voltammograms (first cycle) on BDD anodes of sodium sulfate/sodium hydroxide solutions (pH 12) containing (1) 1.10 mM MCP; (2) 1.10 mM DCP and (3) 1.10 mM TCP. Scan rate 50 mV s^{-1}. Auxiliary electrode: Stainless steel AISI 304. Reference electrode: SCE.

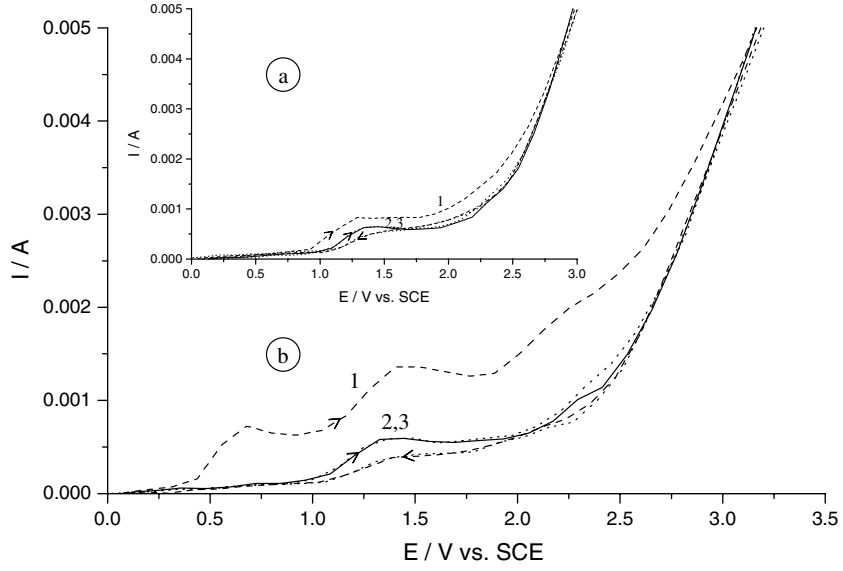

Fig. 4. Cyclic voltammograms on BDD anodes of MCP solutions on sodium sulfate media (5000 mg dm^{-3}) at pH 2 (a) and 12 (b). Scan rate 100 mV s^{-1}. (1) 1st cycle; (2) 2nd cycle and (3) 3rd cycle. Auxiliary electrode: Stainless steel AISI 304. Reference electrode: SCE.

peaks increase in size and are shifted positively as the scan rate increases, again indicating irreversible processes. The third peak (p2) is partially overlapped with oxygen evolution and this situation becomes more marked at higher scan rates as a consequence of the shift to the right. Linear sweep voltammograms for different concentrations of MCP are shown in Figure 6. The peaks increase in size with concentration and the oxidation potential does not change. Similar behaviour was observed for DCP and TCP.

On the basis of these results, it is apparent that the anodic oxidation of the three CPs studied share the same initial reaction stages, as indicated by the presence of the same anodic oxidation peaks [9]. The decrease in size of the peaks with the number of scans can be explained in terms of the production of polymeric materials that decrease electrode activity (electrode fouling). Evidence for this was provided by the delay in the oxygen evolution potential upon increasing CP concentration, with the effect being more marked at alkaline pH. The increase in peak size and their shift to the oxygen evolution region with increasing scan rate both indicate that these peaks correspond to irreversible reactions. Likewise, the decrease in size of the reverse peaks,

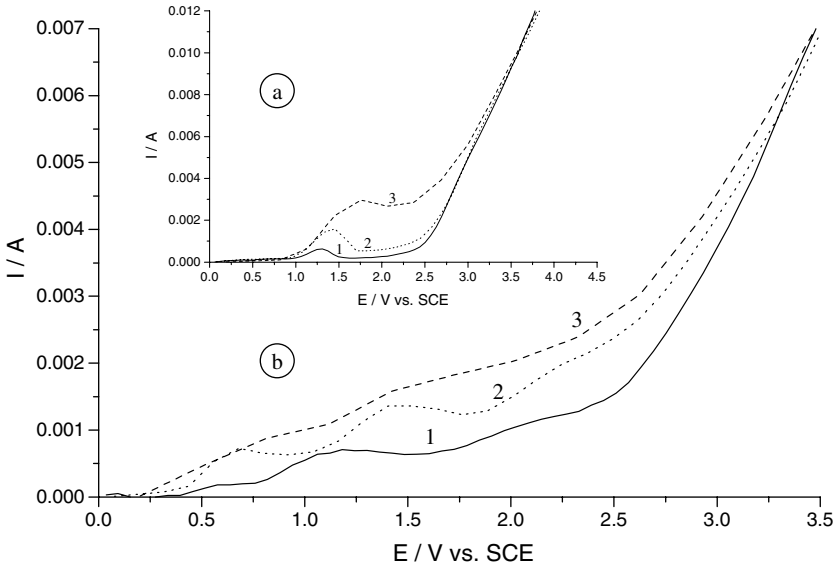

Fig. 5. Linear sweep voltammograms on BDD anodes of MCP solutions on sodium sulfate media (5000 mg dm^{-3}) at pH 2 (a) and 12 (b). Scan rates (1) 50, (2) 100 and (3) 250 mV s^{-1}. Auxiliary electrode: Stainless steel AISI 304. Reference electrode: SCE.

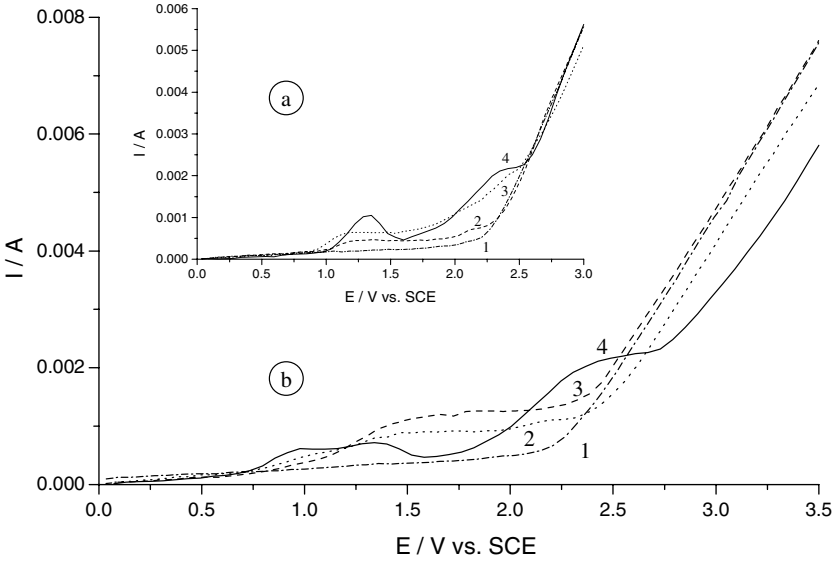

Fig. 6. Linear sweep voltammograms on BDD anodes of MCP solutions on sodium sulfate media (5000 mg dm^{-3}) at pH 2 (a) and 12 (b). Concentrations of MCP: (1) 0, (2) 150, (3) 500 and (4) 1500 mg dm^{-3}. Scan rate 50 mV s^{-1}. Auxiliary electrode: Stainless steel AISI 304. Reference electrode: SCE.

corresponding to peaks p1 and p2, suggests the existence of a later chemical reaction involving the electrochemically formed products (EC mechanism).

These facts are in agreement with literature data [11, 13] and seem to indicate that both peaks (p1 and p2) correspond to the oxidation of chlorophenol to the chlorophenoxy radical and its subsequent oxidation to the chlorophenoxy cation.

It has been reported that the two electrochemically formed compounds are very reactive and can couple to form polymers [15] or undergo other chemical transformations such as: (i) the addition of hydroxyl groups (from water or hydroxyl radicals generated in the potential region of water decomposition) to form chlorodihydroxybenzenes [16–18] and, (ii) the release of chlorine (by substitution with hydroxyl groups) to form non-chlorinated phenolic [16–18] or quinonic intermediates [11, 16, 17]. The occurrence of these reactions can be explained in terms of the suggested EC mechanism. As discussed below (Section 3.2), all these compounds are detected in the electrolysis of the synthetic wastes under investigation.

CPs are weak acids with p*K*a values of 9.45, 7.85 and 6.15 for MCP, DCP and TCP, respectively [3, 19]. At pH 12 almost all CPs are therefore dissociated and peak p1 does not correspond to the oxidation of CP but to the oxidation of chlorophenolate to the chlorophenoxy radical. As a consequence the p1 peak potential is

shifted to slightly higher potentials (+0.2 V) at higher pH.

Voltammetric experiments on alkaline solutions containing CP show an additional peak (p3) and this is close to p1. The size of p3 increases on addition of chloride ions and hydroquinone to the solution. This fact, together with the observation of chloride ions in strongly alkaline solutions of CPs, indicates the existence of the chemical substitution of chloride by hydroxyl groups [20]. Peak p3 could therefore correspond to the oxidation of the phenolic to the quinonic form.

A peak (p4) that may correspond to the reduction of this quinonic form (−0.30 V vs SCE) is shown in Figure 7(a) along with a new peak (p5) close to the hydrogen evolution potential (−1.78 V vs SCE). A new cycle leads to an increase in the size of p1 and the presence of a new anodic oxidation peak (p6) at 1.80 V vs SCE. This peak is due to the oxidation of chlorides, as can be seen in Figure 7(b). Thus, p5 can be interpreted as being due to the cathodic hydrodehalogenation (HDH) of the CP to give less-chlorinated phenolic species.

The increase in peak p1 can be interpreted as being due to the oxidation of the newly formed species. Thus, if a small amount of phenol is added to a solution of MCP at the beginning of the second cycle of a cyclic voltammetry experiment, a similar shift in p1 and an increase in the measured current density is observed. The decrease in the peak size in the second cycle when the lower voltage is 0 V vs SCE (as compared to those obtained when the lower voltage is close to hydrogen evolution) indicates destruction of the polymeric layer.

The HDH of the different chlorophenols on commercial stainless steel (SS) AISI 304 (the cathode used in this work) was confirmed by performing a number of linear voltammetric sweeps (Figure 8). Hydrogen evolution appears at a lower (absolute value) overpotential with SS and so the HDH peak is hidden by hydrogen evolution. Nevertheless, the existence of this reaction is confirmed by the positive shift in the hydrogen evolution potential when CPs are present in solution. This shift becomes more marked as the number of chloro-substituents in the CP molecule increases, a fact suggesting complete HDH of the CPs.

3.2. *General behaviour in galvanostatic electrolysis*

The oxidation process of the CPs under investigation were compared by carrying out galvanostatic electrolysis assays on samples containing the same concentrations (1.10 mmol dm^{-3}) of the compounds. The curves for the variation of TOC vs the specific electrical charge passed are shown in Figure 9. Complete mineralization of the waste occurs and a complex shape is obtained with a plateau that decreases in size with the number of chloro-substituents in the oxidized molecule. The initial mineralization rate decreases with the number of chloro-substituents in the CP, although the process ends at practically the same value of specific electrical charge passed.

The variations of the main carbon compounds in the oxidation process with the specific electrical charge passed are shown in Figures 10(a), 11(a) and 12(a). The electrochemical oxidation of CPs on BDD electrodes leads to the formation of carbon dioxide and volatile

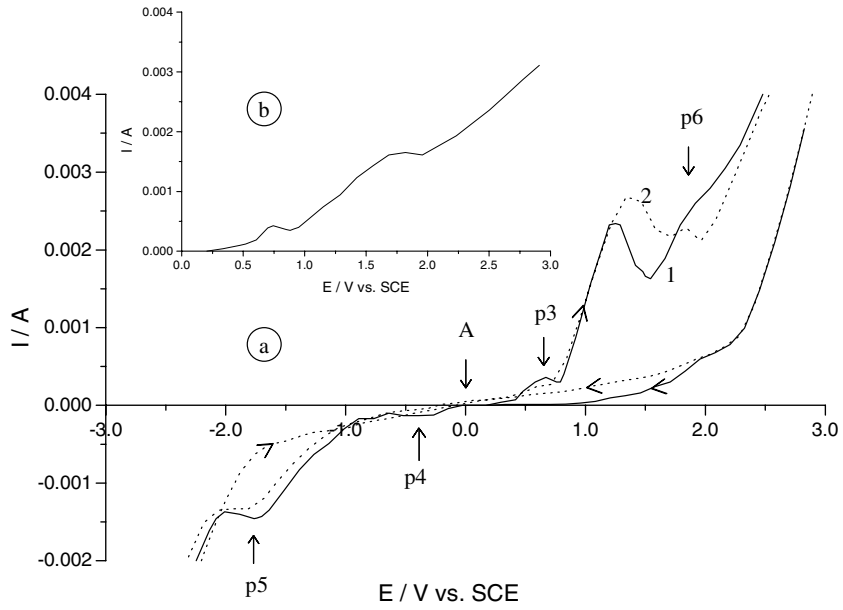

Fig. 7. Characterization of peak p3. (a) Cyclic voltammograms on BDD anodes of MCP solutions on sodium sulfate/sodium hydroxide media (pH 12, 5000 mg dm^{-3}) (1) 1st cycle and (2) 2nd cycle. Auxiliary electrode: Stainless steel AISI 304. Reference electrode: SCE. Scan rate 100 mV s^{-1}. A: Anodic start of the CV. (b) Linear sweep voltammograms on BDD anodes of sodium sulfate/sodium hydroxide solutions containing 10 mg dm^{-3} of chloride ions.

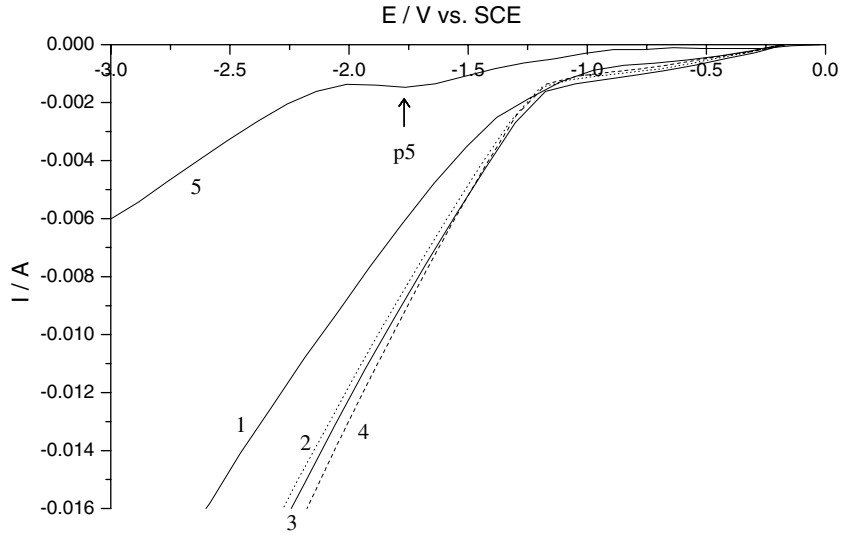

Fig. 8. Linear sweep voltammograms on SS (AISI 304) and BDD cathodes of sodium hydroxide/sodium sulfate solutions (5000 mg dm^{-3} Na_2SO_4; pH 12) containing: (1) no organic matter, SS cathode; (2) 500 mg dm^{-3} of MCP, SS cathode; (3) 5 mg dm^{-3} DCP, SS cathode; (4) 500 mg dm^{-3} of TCP, SS cathode and (5) 500 mg dm^{-3} of MCP, BDD anode. Scan rate 100 mV s^{-1}. Auxiliary electrode: Stainless steel AISI 304. Reference electrode: SCE.

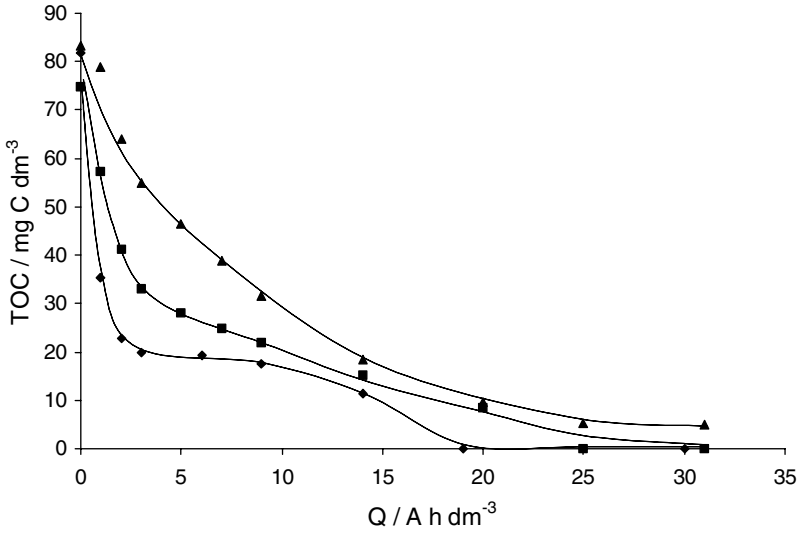

Fig. 9. Decrease of TOC with the specific electrical charge passed ($n^0 = 1.1$ mM; pH 2; $T = 25$ °C; $\rho = 30$ mA cm^{-2}). (♦) MCP; (■) DCP; (▲) TCP.

chlorinated organic compounds, mainly chloroform, as the final products. The main organic intermediate formed in every case (identified by HPLC) is oxalic acid, along with lower concentrations of maleic and fumaric acids. Chlorinated intermediates were not detected in these electrolysis assays and the intermediates observed are the same as those typically obtained in the electrochemical oxidation of phenolic aqueous wastes [21–24].

The inorganic carbon (IC) plot also has a complex shape due to the formation of oxalic acid, which delays the generation of carbon dioxide and causes the appearance of the plateau because of its low oxidizability [25, 26]. The plateau corresponds to the increase in the concentration of oxalic acid (Figures 10(a), 11(a) and 12(a)).

Chloride and hypochlorite were also detected in the system and were quantified by ion chromatography. The variation of these components is shown in Figures 10(b), 11(b) and 12(b). Both species show typical intermediate behaviour since chloride can be transformed into hypochlorite, which is either oxidized or combines with organic materials. The concentration of oxidants (measured by an I^-/I_2 test) is also shown. A similar trend is observed for the hypochlorite measurements. The total concentration of hypochlorite can not fully account for the measured concentration of oxidizing compounds, indicating that other oxidants are formed. It has been proposed [27] that peroxodisulphates can be formed in the electrochemical oxidation with BDD electrodes of wastes containing sulphates (Equation 1). These

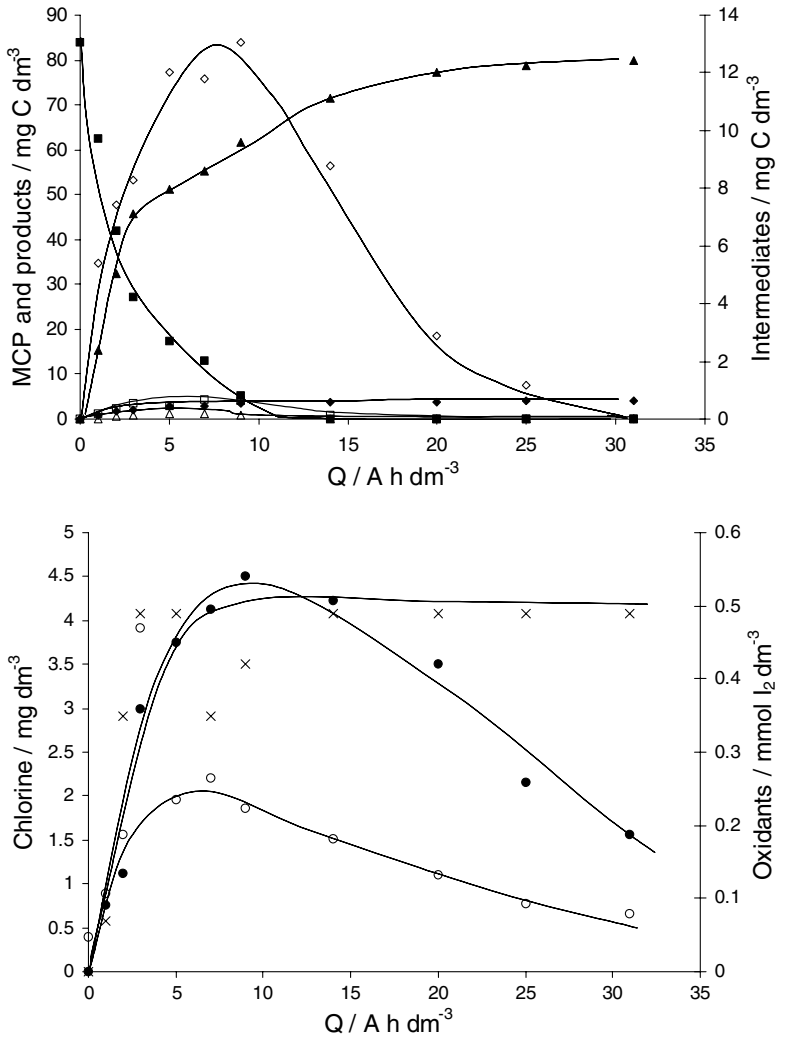

Fig. 10. Concentration change of 4-chlorophenol, intermediates and products obtained, chlorine and oxidants with the specific electrical charge passed ($n^0 = 1.1$ mM; pH 2; $T = 25$ °C; $\rho = 30$ mA cm^{-2}). Key: (■) MCP; (▲) CO_2; (♦) volatile chlorinated organic compounds; (◇) oxalic acid; (□) maleic acid; (△) fumaric acid; (○) Cl^-; (●) ClO^- and (**x**) oxidant reagent (mM of I_2).

compounds are very powerful oxidants and can attack organic matter. The decomposition of peroxodisulphates gives hydrogen peroxide and other oxidants [26, 28], meaning that several oxidizing agents could be involved in the mediated processes.

$$2\,SO_4^{2-} \longrightarrow S_2O_8^{2-} + 2\,e^- \qquad (1)$$

Mediated oxidation by hypochlorite, peroxodisulphates and other inorganic reagents electrogenerated on the electrode surface must be considered in the global oxidation process along with direct oxidation occurring on the electrode surface.

The relationship between the mediated oxidation and the operating conditions (temperature and current density) and electrolyte composition (pH, concentration and supporting media) is discussed in Part II of this work.

To obtain comparable results between the three CPs, and given the low solubility of TCP in water, the previously described experiments were applied to low concentrations of DCP and MCP. Further information concerning intermediates was obtained from experiments with higher MCP and DCP concentrations (27.8 mmol dm^{-3}). The maximum concentrations of organic intermediates in these experiments are shown in Table 2. The same compounds were detected as in the low concentration electrolysis assays. In addition, hydroquinone, benzoquinone and formic and trichloroacetic acids were detected in significant concentrations. Trichloroacetic is converted to the unstable trichloroacetate at alkaline pH and this rapidly decomposes to VOC. TCA was therefore not detected at pH 12. Other chlorinated aromatics (chlororesorcinol and chlorohydroquinone) were also detected, but these were only present in very low concentrations (close to HPLC detection limits).

Identification of the intermediates in the galvanostatic electrolysis of CPs (including the compounds and their appearance times), together with information obtained from the voltammetric study, allows the development of a simple mechanistic model (Figure 13).

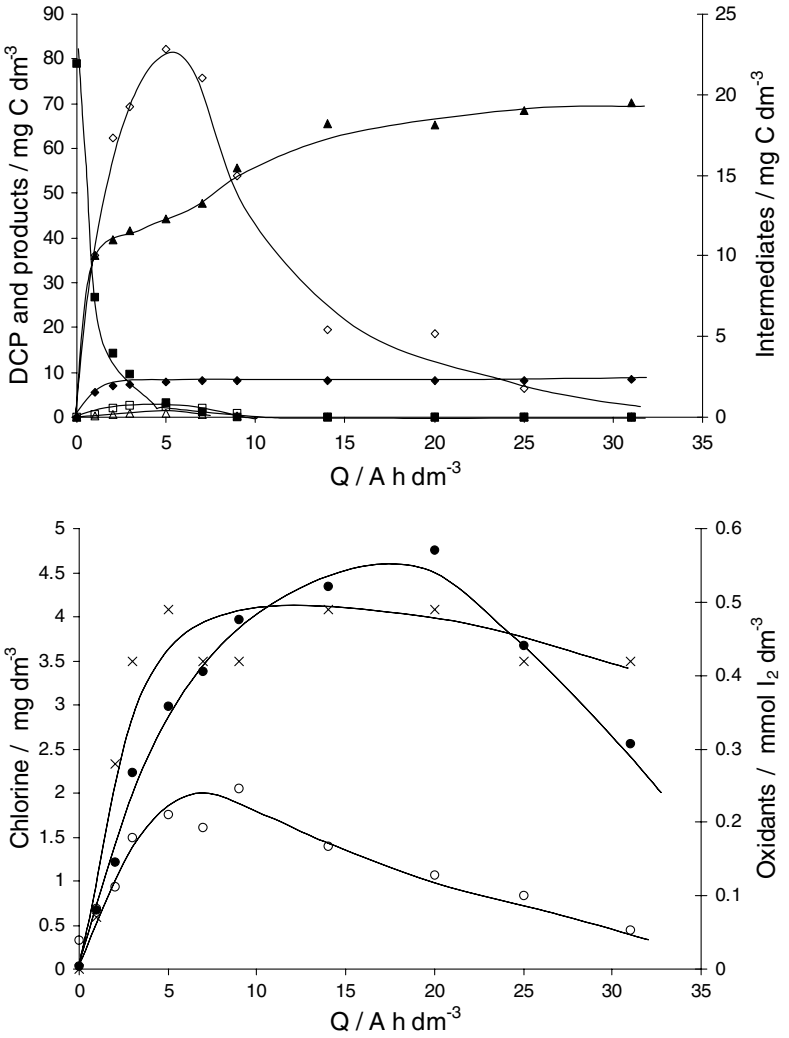

Fig. 11. Concentration change of 2,4-dichlorophenol, intermediates and products obtained, chlorine and oxidants with the specific electrical charge passed ($n^0 = 1.1$ mM; pH 2; $T = 25$ °C; $\rho = 30$ mA cm^{-2}). Key: (■) DCP; (▲) CO_2; (◆) volatile chlorinated organic compounds; (◇) oxalic acid; (□) maleic acid; (△) fumaric acid; (○) Cl^-; (●) ClO^- and (**x**) oxidant reagent (mM of I_2).

The electrochemical treatment of CPs initially leads to anodic and/or cathodic HDH of the CP to give non-chlorinated phenolic (P) and quinonic compounds (Q) along with chloride ions (Cl^-). Aromatic ring cleavage then occurs to give C_4 (fumaric and maleic), C_2 (oxalic) and C_1 (formic) dicarboxylic acids. Chlorine arising from the HDH of the CPs are converted at the anode into more oxidized species (Cl^-) and these can react with the unsaturated C_4 carboxylic acid to yield trichloroacetic acid (TCA) through a haloform reaction [29]. The non-chlorinated organic acids are finally oxidized to carbon dioxide and the trichloroacetic acid into carbon dioxide and volatile organo-chlorinated molecules (VOC). The oxidation processes in this model can occur either directly on the electrode surface or are mediated by hypochlorite, peroxodisulphate and other inorganic reagents electrogenerated at the electrode surface.

This simple model not only explains the presence of particular compounds but is also consistent with the time evolution of the different intermediates. In the experiments involving low initial concentrations (Figures 10, 11 and 12), the maximum concentration of C_4 dicarboxylic acids decreases on increasing the number of chloro-substituents in the CP molecule. In addition, the maximum concentration of oxalic acid is reached at lower Q values for highly substituted CPs.

In the experiments involving high initial concentrations (Table 2), MCP gives rise to higher concentrations of maleic and fumaric acids than oxalic acid, but this trend is opposite for DCP. This situation occurs because highly chlorinated CPs release larger amounts of chlorine and this, once oxidized, quickly combines with C_4 dicarboxylic acids to form trichloroacetic acid. Consequently, the concentration of maleic and fumaric acids in solution decreases and, therefore, so does the amount of oxalic acid that can be formed by their oxidation.

4. Conclusions

The following conclusions can be drawn:

(i) Electrochemical oxidation can successfully treat MCP, DCP and TCP aqueous wastes. In each case,

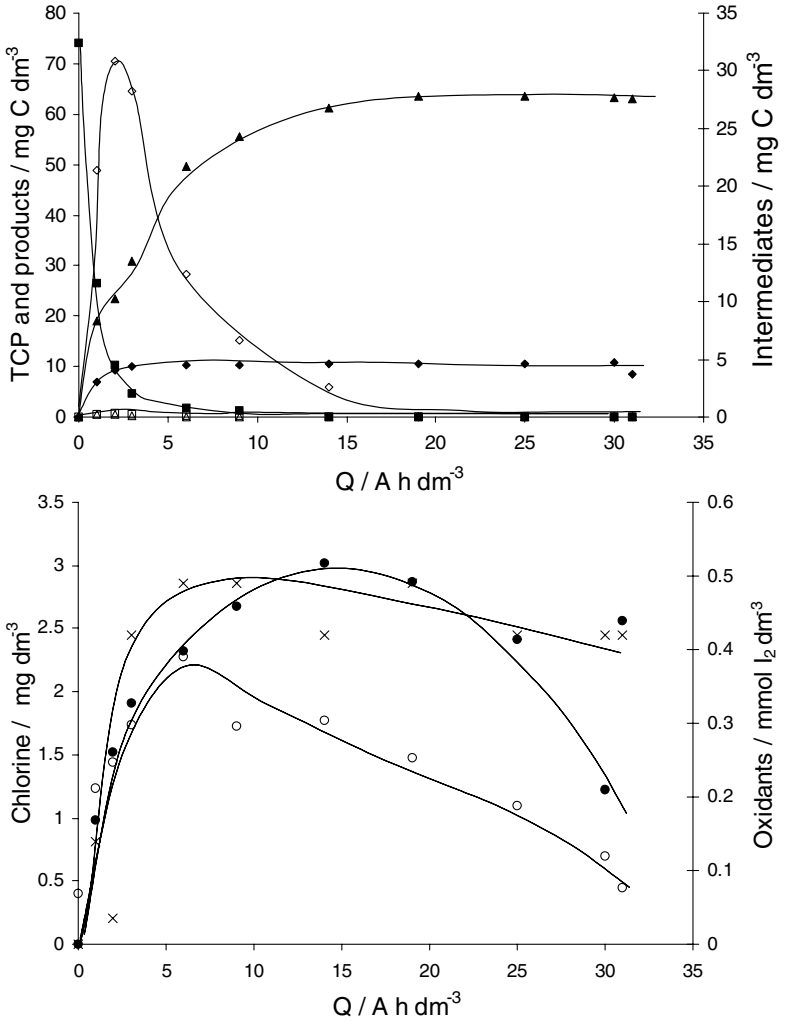

Fig. 12. Concentration change of 2,4,6-trichlorophenol, intermediates and products obtained, chlorine and oxidants with the specific electrical charge passed ($n^0 = 1.1$ mM; pH 2; $T = 25$ °C; $\rho = 30$ mA cm^{-2}). Key: (■) TCP; (▲) CO_2; (♦) volatile chlorinated organic compounds; (◇) oxalic acid; (□) maleic acid; (△) fumaric acid; (○) Cl^-; (●) ClO^- and (**x**) oxidant reagent (mM of I_2).

Table 2. Maximum concentrations measured (referred to the initial carbon concentration) for the main aromatic and carboxylic acid intermediates detected in the galvanostatic electrolysis of solutions containing 27.8 mmol dm^{-3} of MCP and DCP

Intermediates	MCP		DCP	
	pH 2	*pH 12*	*pH 2*	*pH 12*
Hydroquinone	1.95	11.42	0.52	0.00
Benzoquinone	0.00	6.11	0.00	0.00
Fumaric acid	0.28	3.38	0.39	0.34
Maleic acid	10.16	8.09	1.54	2.69
Trichloroacetic acid	1.99	0.00	4.21	0.00
Oxalic acid	5.74	4.89	6.75	6.67
Formic acid	4.15	4.83	0.00	2.27

complete conversion of the organic pollutants into carbon dioxide and volatile chlorinated organic compounds (mainly chloroform) was achieved.

(ii) The main intermediates formed in the oxidation processes were hydroquinone, maleic, fumaric and oxalic acids. Other carboxylic acids (formic and trichloroacetic) and very small amounts of chlorinated aromatic intermediates (such as chlorohydroquinone and chlororesorcinol) were also detected in low concentrations. CPs were found to release chloride ions during the electrolytic process and these were oxidized to species with higher oxidation states.

(iii) A simple mechanistic model is consistent with the results obtained in this study. According to this model, the electrochemical treatment of CP aqueous wastes leads initially to the anodic and cathodic release of

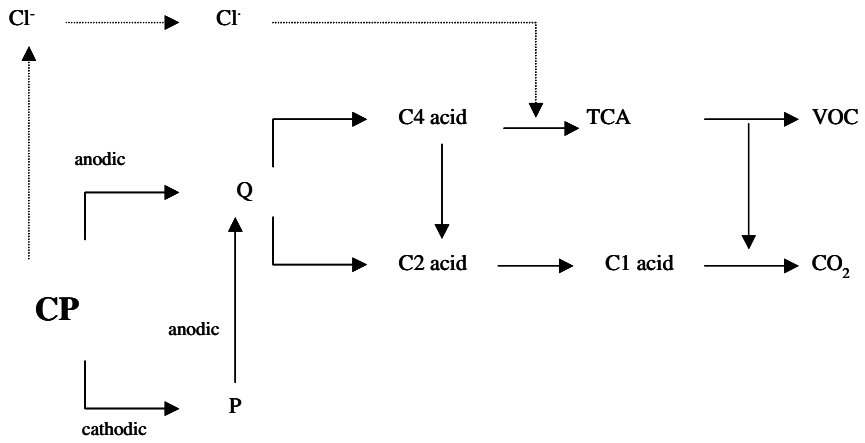

Fig. 13. Sketch of the simple mechanistic model proposed to explain the main processes occurring in the electrochemical treatment of CP wastes using BDD anodes.

chlorine and to the formation of non-chlorinated aromatic intermediates. Aromatic ring cleavage then occurs and C_4, C_2 and C_1 dicarboxylic acids are formed. Chlorine arising from the HDH of the CPs is converted at the anode into more oxidized species that can react with unsaturated C_4 carboxylic acid to yield trichloroacetic acid through a haloform reaction. The non-chlorinated organic acids are finally oxidized to carbon dioxide, and the trichloroacetic acid into carbon dioxide and volatile organo-chlorinated molecules.

(iv) Both direct and mediated electrochemical oxidation processes occur in the electrochemical treatment of CPs. Inorganic reagents electrogenerated at the electrode surface – such as hypochlorite and peroxodisulphates – play an important role in the global oxidation process.

Acknowledgements

This work was supported by the MCT (Ministerio de Ciencia y Tecnología, Spain) and by the EU (European Union) through the Project REN2001-0560. The Contribution of Junta de Comunidades de Castilla-La Mancha (Consejería de Ciencia y Tecnología) is also acknowledged.

References

1. T.L. Ho and J.R. Bolton, *Wat. Res.* **30** (1998) 489.
2. T.M. Martin and D.M. Young, *Chem. Res. Toxicol.* **14** (2001) 1378.
3. T. Kishino and K. Kobayshi, *Wat. Res.* **30** (1996) 393.
4. U. Leffrang, K. Ebert, K. Flory, U. Galla and H. Schmieder, *Sep. Sci. Technol.* **30** (1995) 1883.
5. A.M. Polcaro and S. Palmas, *Ind. Eng. Chem. Res.* **36** (1997) 1791.
6. A.M. Polcaro, S. Palmas, F. Renoldi and M. Mascia, *J. Appl. Electrochem.* **29** (1999) 147.
7. M. Gatrell and B. MacDougall, *J. Electrochem. Soc.* **146** (1999) 3335.
8. S.K. Johnson, L.L. Houk, J. Feng, R.S. Houk and D.C. Johnson, *Environ. Sci. Technol.* **33** (1999) 2638.
9. J.D. Rodgers, W. Jedral and N.J. Bunce, *Environ. Sci. Technol.* **33** (1999) 1453.
10. M.O. Azzam, M. Al-Tarazi and Y. Tahboub, *J. Haz. Mater.* **B75** (2000) 99.
11. M.A. Rodrigo, P.A. Michaud, I. Duo, M. Panizza, G. Cerisola and Ch. Comninellis, *J. Electrochem. Soc.* **148** (2001) D60.
12. L. Gherardini, P.A. Michaud, M. Panizza, Ch. Comninellis and N. Vatistas, *J. Electrochem. Soc.* **148** (2001) D78.
13. M.S. Ureta-Zañartu, P. Bustos, C. Berríos, M.C. Diez, M.L. Mora and C. Gutiérrez, *Electrochim. Acta* **47** (2002) 2399.
14. A. de Lucas, P. Cañizares, M.A. Rodrigo, J. Garcia-Gomez, 'Waste Management 2002' (WIT Press, Southampton, UK, 2002) p. 771.
15. Ch. Comninellis and C. Pulgarín, *J. Appl. Electrochem.* **21** (1991) 703.
16. S. Basu and I.W. Wei, *Environ. Eng. Sci.* **17** (2000) 279.
17. J. Theurich, M. Lindner and D.W. Bahnemann, *Langmuir* **12** (1996) 6368.
18. T. Pandiyan, O. Martínez-Rivas, J. Orozco-Martínez, G. Burillo Amescua and M.A. Martínez-Carrillo, *J. Photochem. Photobiol. A: Chem.* **146** (2002) 149.
19. C.D. Adams, R.A. Cozzens and B.J. Kim, *Wat. Res.* **31** (1997) 2655.
20. K. Vollhardt and C. Peter, 'Organic Chemistry' (W.H. Freeman & Co., New York, 1994), p. 1156.
21. Ch. Comninellis, *Trans. IchemE.* **70(B)** (1992) 219.
22. Ch. Comninellis, *Electrochim. Acta* **39** (1994) 1857.
23. G. Foti, D. Gandini, Ch. Comninellis, A. Perret and W. Haenni, *Electrochem. Solid-State Lett.* **2** (1999) 228.
24. P. Cañizares, M. Diaz, J.A. Dominguez, J. Garcia-Gomez and M.A. Rodrigo, *Ind. Eng. Chem. Res.* **41** (2002) 4187.
25. J. Iniesta, P.A. Michaud, M. Panizza, G. Gerisola, A. Aldaz and Ch. Comninellis, *Electrochim. Acta* **46** (2001) 3573.
26. P. Cañizares, J. Lobato, J. García-Gómez and M.A. Rodrigo, *Ind. Eng. Chem. Res.* **42** (2003) 956.
27. P.A. Michaud, E. Mahé, W. Haenni, A. Perret and Ch. Comninellis, *Electrochem. Solid-State Lett.* **3** (2000) 77.
28. P.A. Michaud, Ch. Comninellis, W. Haenni, A. Perret, J. Iniesta, M. Fryda and L. Schaefer, *in* 'Energy and Electrochemical Processes for a Cleaner Environment', Proceedings Volume 2001-23 (Electrochemical Society, NJ, 2001), p. 87.
29. R.A. Larson and E.J. Weber, 'Reaction Mechanisms in Environmental Organic Chemistry', (CRC Press, Boca Raton, 1994), p. 433.